
Figures and figure supplements

Schnyder corneal dystrophy-associated UBIAD1 inhibits ER-associated degradation of HMG CoA reductase in mice

Youngah Jo et al

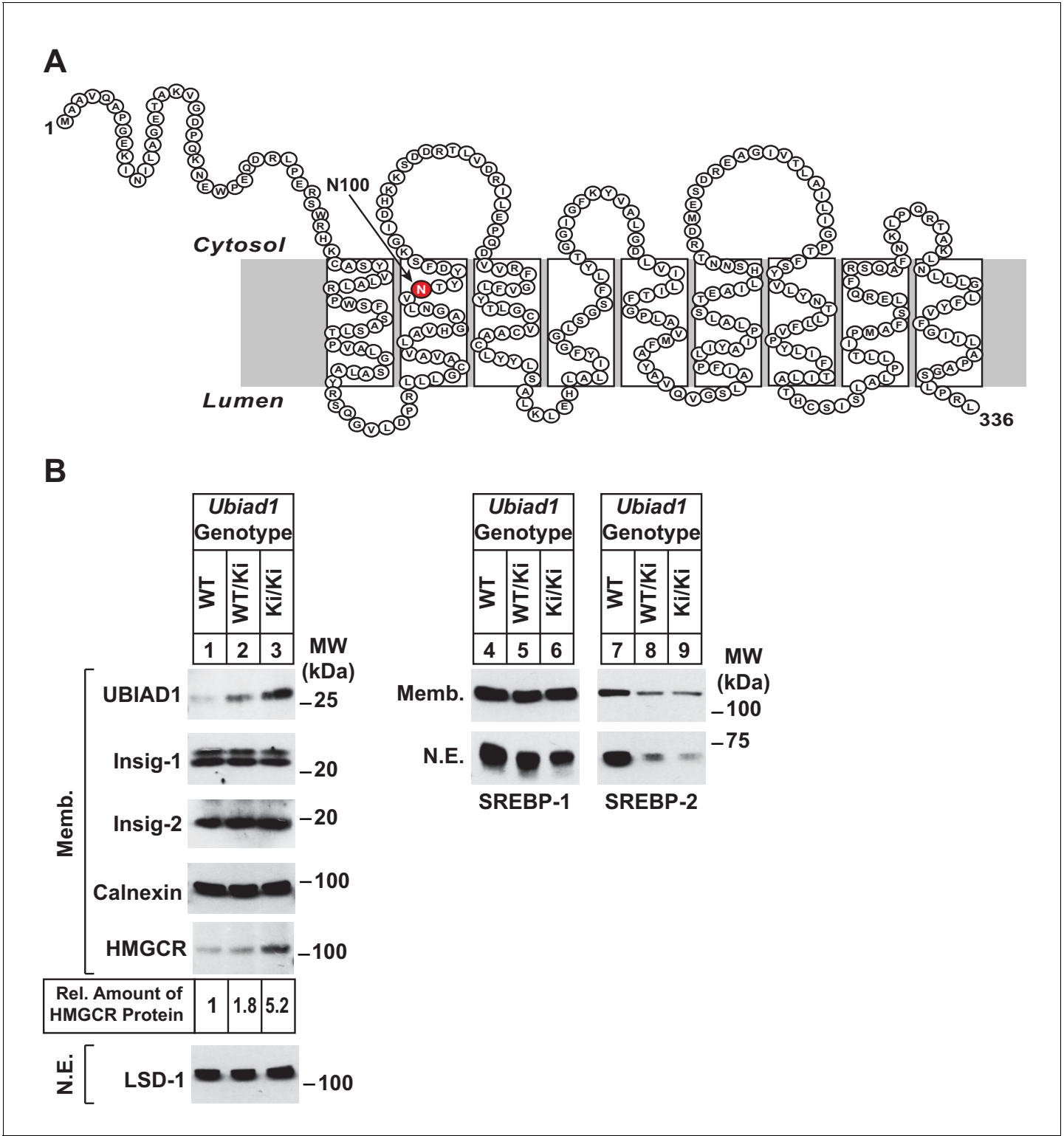


Figure 1. Accumulation of HMGCR protein in livers of *Ubiad1*^{Ki/Ki} mice with mixed C57BL/6 × 129 genetic background. (A) Amino acid sequence and predicted topology of mouse UBIAD1 protein. Asparagine-100 (N100), which corresponds to the most frequently mutated amino acid residue in SCD, is enlarged, shaded in red and indicated by an arrow. (B) Male WT, *Ubiad1*^{WT/Ki}, and *Ubiad1*^{Ki/Ki} littermates (8–9 weeks of age, eight mice/group) were fed an *ad libitum* chow diet prior to sacrifice. Livers of the mice were harvested and subjected to subcellular fractionation as described in ‘Materials and methods.’ Aliquots of resulting membrane (Memb.) and nuclear extract (N.E.) fractions (80–160 μg of total protein/lane) for each group were pooled and subjected to SDS-PAGE, followed by immunoblot analysis using antibodies against endogenous HMGCR, SREBP-1, SREBP-2, UBIAD1, Insig-1, Figure 1 continued on next page

Figure 1 continued

Insig-2, calnexin, and LSD-1. Although shown in a separate panel, LSD-1 serves as a loading control for the nuclear SREBP immunoblots. The amount of hepatic HMGCR protein in *Ubiad1*^{Ki/Ki} mice was determined by quantifying the band corresponding to HMGCR using ImageJ software.

DOI: <https://doi.org/10.7554/eLife.44396.002>

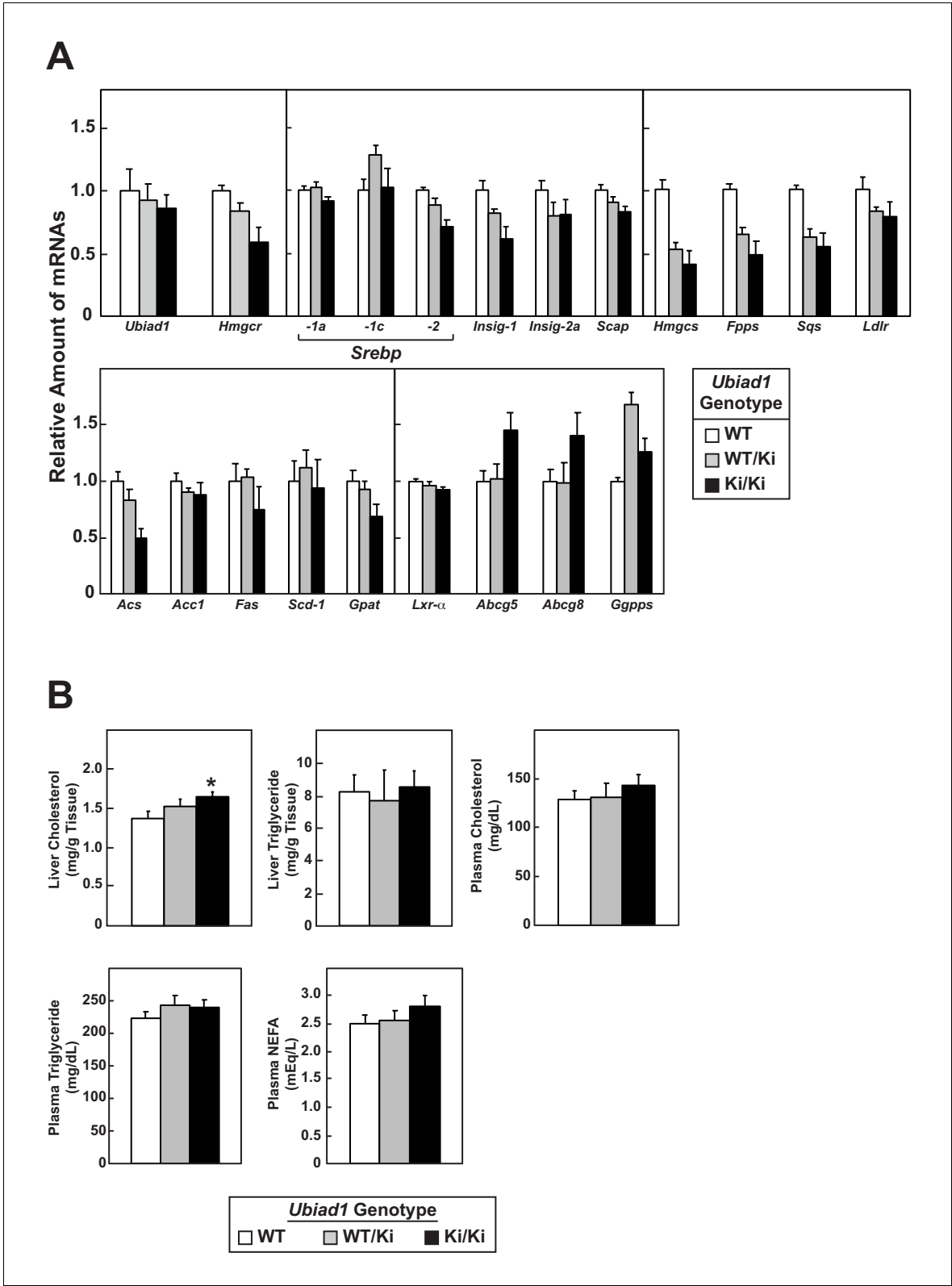


Figure 1—figure supplement 1. Relative amounts of hepatic mRNAs encoding components of the Scap-SREBP pathway and lipid analysis in WT and *Ubiad1*^{Ki/Ki} mice. (A) Total RNA isolated from livers of mice used in **Figure 1B** (8 mice/group) was separately isolated. Equal amounts of RNA from the individual mice were subjected to quantitative real-time RT-PCR using primers against the indicated gene; cyclophilin mRNA was used as an invariant control. Each value represents the amount of mRNA relative to that in WT mice, which is arbitrarily defined as 1. Bars, mean ± S.E. (error bars) of data

Figure 1—figure supplement 1 continued on next page

Figure 1—figure supplement 1 continued

from eight mice. (B) The amount of cholesterol, triglycerides, and non-esterified fatty acids (NEFA) in livers and plasma from WT or *Ubiad1* knockin mice used in **Figure 1B** was determined by a colorimetric assay as described in 'Materials and methods.' Error bars, S.E. The *p* value was calculated using Student's *t* test: *, $p \leq 0.05$. *Hmgcs*, HMG coenzyme A synthase; *Fpps*, farnesyl pyrophosphate synthase; *Sqs*, squalene synthase; *Acs*, acetyl coenzyme A synthetase; *Acc1*, acetyl coenzyme A carboxylase-1; *Fas*, fatty acid synthase; *Scd-1*, stearyl coenzyme A desaturase-1; *Gpat*, glycerol-3-phosphate acyltransferase; *Abcg5* and *Abcg8*, ATP-binding cassette subfamily G member 5 and 8, respectively; *Ggpps*, geranylgeranyl pyrophosphate synthase.

DOI: <https://doi.org/10.7554/eLife.44396.003>

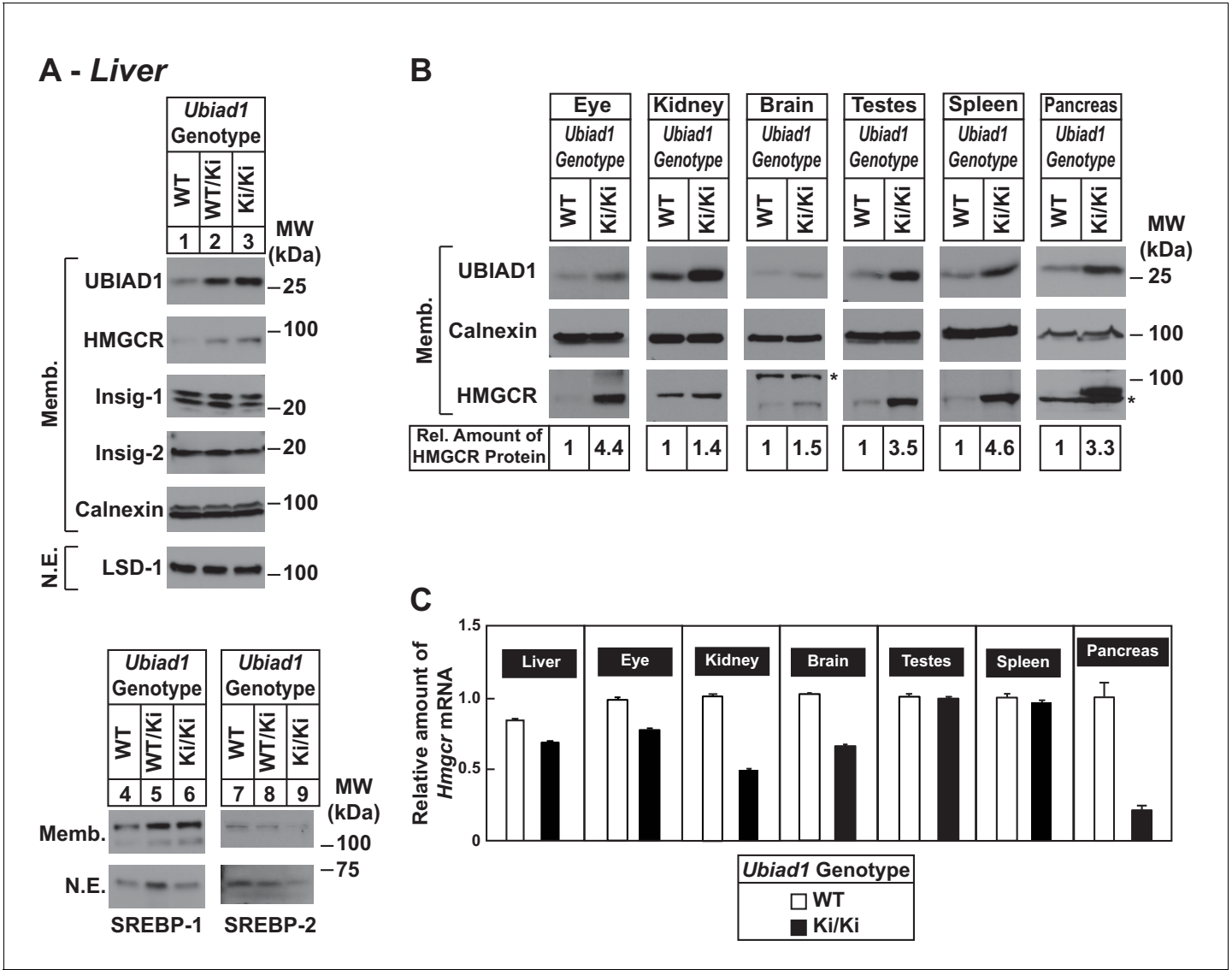


Figure 2. Accumulation of HMGCR protein in tissues of WT and *Ubiad1*^{Ki/Ki} mice with C57BL/6 genetic background. (A and B) Eight to nine-week old male WT, *Ubiad1*^{WT/Ki}, and *Ubiad1*^{Ki/Ki} littermates (six mice/group) were fed an *ad libitum* chow diet prior to study. Aliquots of membrane (Memb.) and nuclear extract (N.E.) fractions from homogenized livers, enucleated eyes, kidneys, brains, testes, and spleens (23–50 µg of total protein/lane) were analyzed by immunoblot using antibodies against the indicated proteins. The asterisk indicates a non-specific cross-reactive band observed in the anti-HMGCR immunoblot from brain and pancreas. Although shown in separate panels, LSD-1 serves as a loading control for the nuclear SREBP-1 and SREBP-2 immunoblots. In (B), the amount of HMGCR protein in the indicated tissues from *Ubiad1*^{Ki/Ki} mice was determined by quantifying the band corresponding to HMGCR using Image J software. (C) For mRNA analysis, equal amounts of RNA from the indicated tissue of individual mice were subjected to quantitative real-time RT-PCR using primers against the *Hmgcr* mRNA and cyclophilin mRNA as an invariant control. Error bars, S.E.
DOI: <https://doi.org/10.7554/eLife.44396.004>

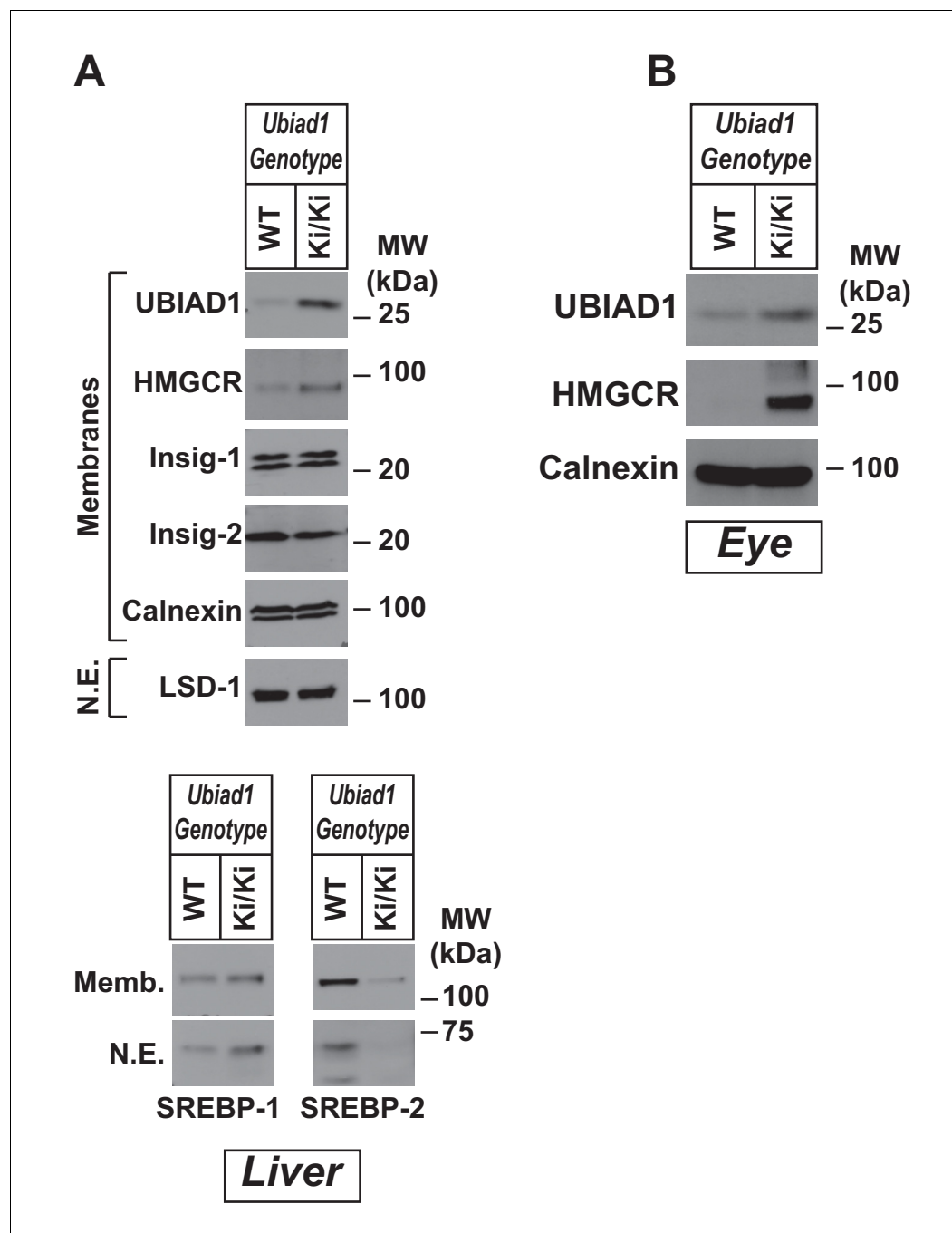


Figure 2—figure supplement 1. Accumulation of HMGCR protein in eyes and livers of WT and *Ubiad1*^{Ki/Ki} mice. Female WT, *Ubiad1*^{WT/Ki}, and *Ubiad1*^{Ki/Ki} littermates of animals used in **Figure 2** (six mice/group, 8–9 weeks of age) were fed an *ad libitum* chow diet prior to study. Aliquots of membrane (Memb.) and nuclear extract (N.E.) fractions from homogenized livers (**A**) and enucleated eyes (**B**) (50–80 µg of total protein/lane) were analyzed by immunoblot using antibodies against the indicated proteins. Although shown in separate panels, LSD-1 serves as a loading control for the nuclear SREBP-1 and SREBP-2 immunoblots in (**A**).

DOI: <https://doi.org/10.7554/eLife.44396.005>

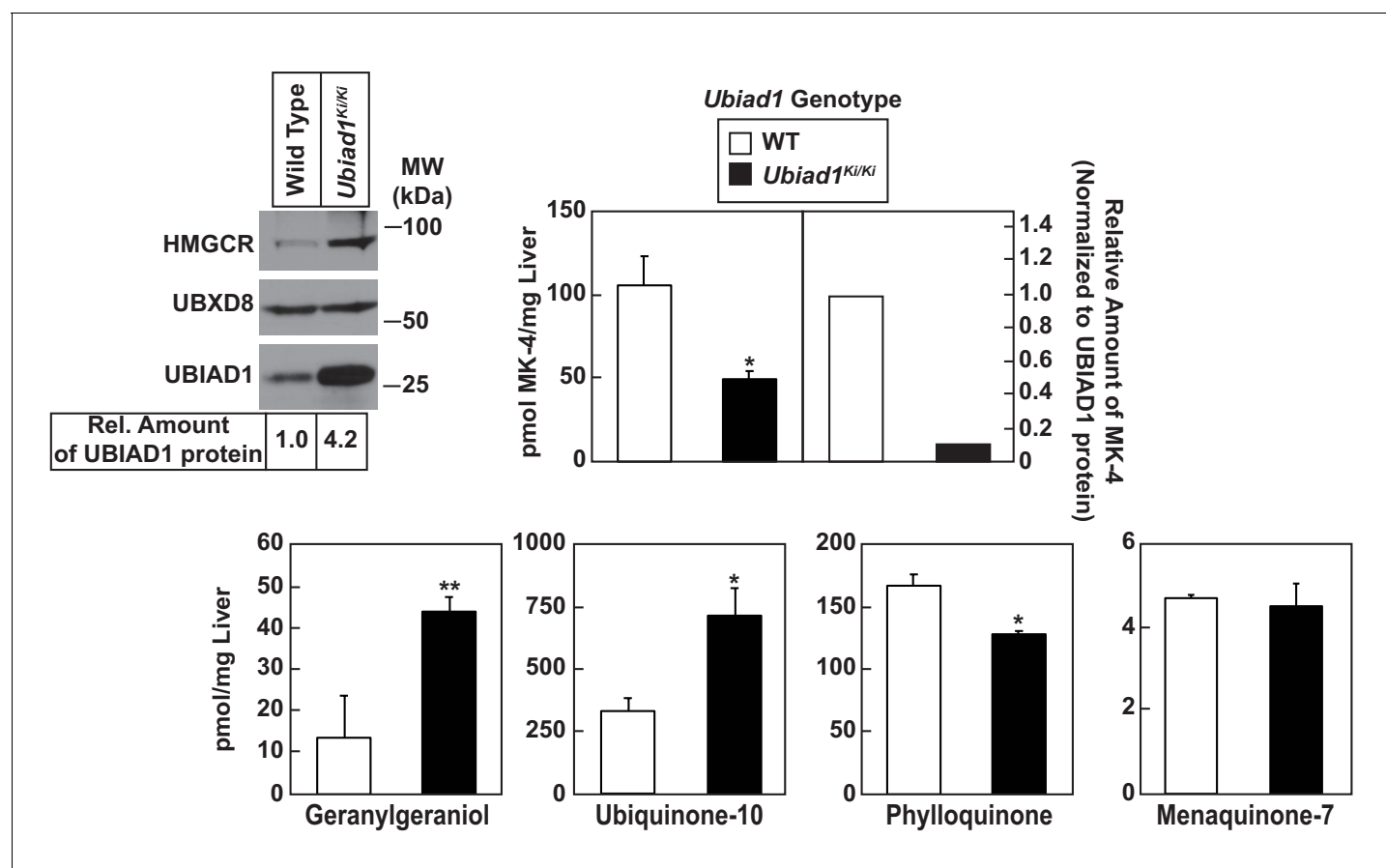


Figure 3. Analysis of nonsterol isoprenoids in WT and *Ubiad1^{Kl/Kl}* mice. Male mice (10–12 weeks of age, five mice/group) were fed *ad libitum* a chow diet prior to study. Livers were collected for subcellular fractionation and immunoblot analysis of resulting membrane fractions (80 μ g total protein/lane) using antibodies against the indicated proteins or to determine the amount of menaquinone-4 (MK-4), geranylgeraniol, ubiquinone-10, phylloquinone, and menaquinone-7 (MK-7) by LC-MS/MS as described in 'Materials and methods.' The relative amount of hepatic MK-4 in *Ubiad1^{Kl/Kl}* mice was determined by normalizing the amount of the vitamin K₂ subtype to the amount of UBIAD1 protein, which was quantified using ImageJ software. Error bars, S.E. The *p* value was calculated using Student's *t* test: *, *p* < 0.05; **, *p* < 0.01.

DOI: <https://doi.org/10.7554/eLife.44396.007>

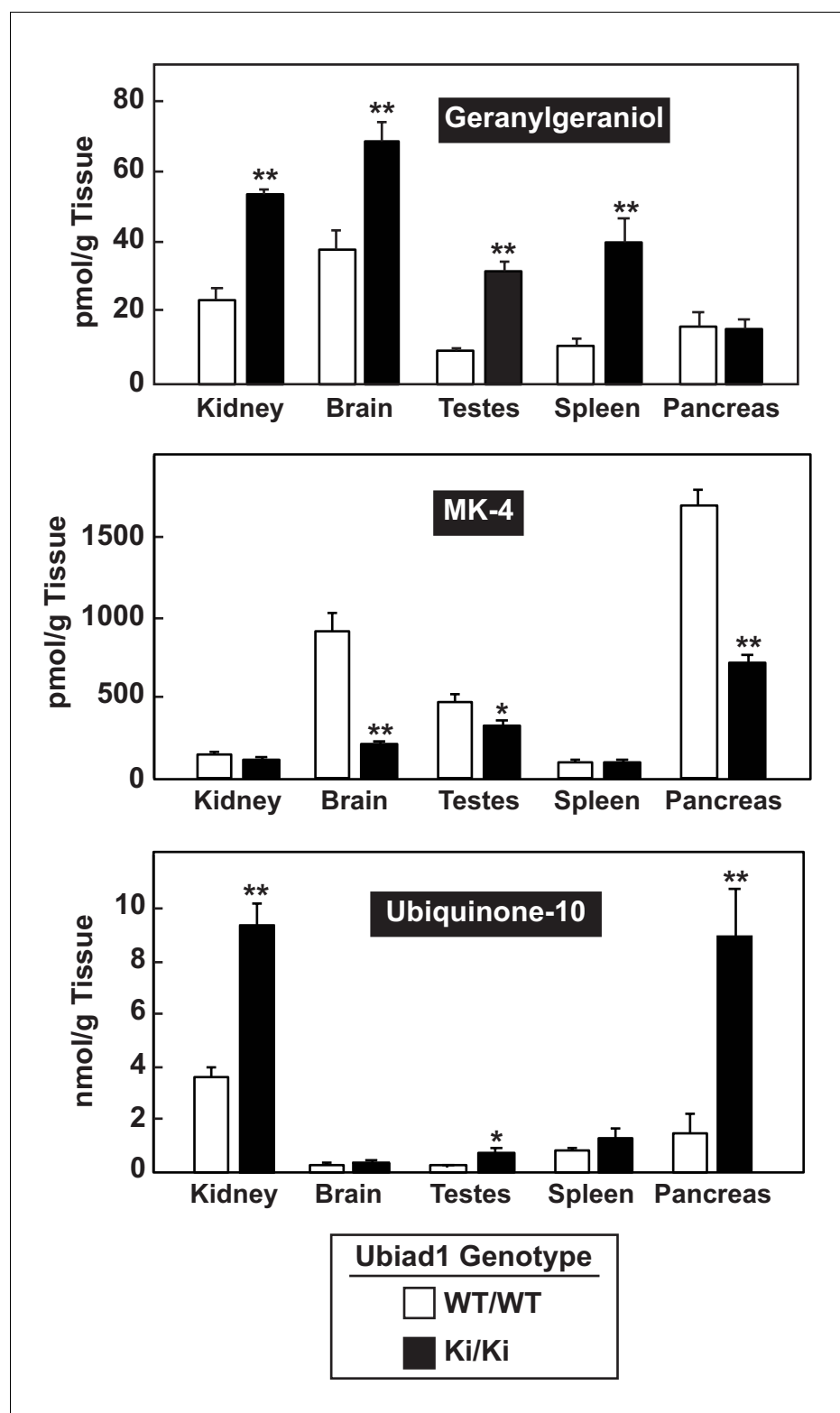


Figure 3—figure supplement 1. Analysis of nonsterol isoprenoids in various tissues of WT and *Ubiad1*^{Ki/Ki} mice. The indicated tissues from mice used in **Figure 3** were collected and the amount of menaquinone-4 (MK-4), geranylgeraniol, and ubiquinone-10 by LC-MS/MS as described in 'Material and methods.' Error bars, S.E. The *p* value was calculated using Student's *t* test: *, *p* < 0.05; **, *p* < 0.01.

DOI: <https://doi.org/10.7554/eLife.44396.008>

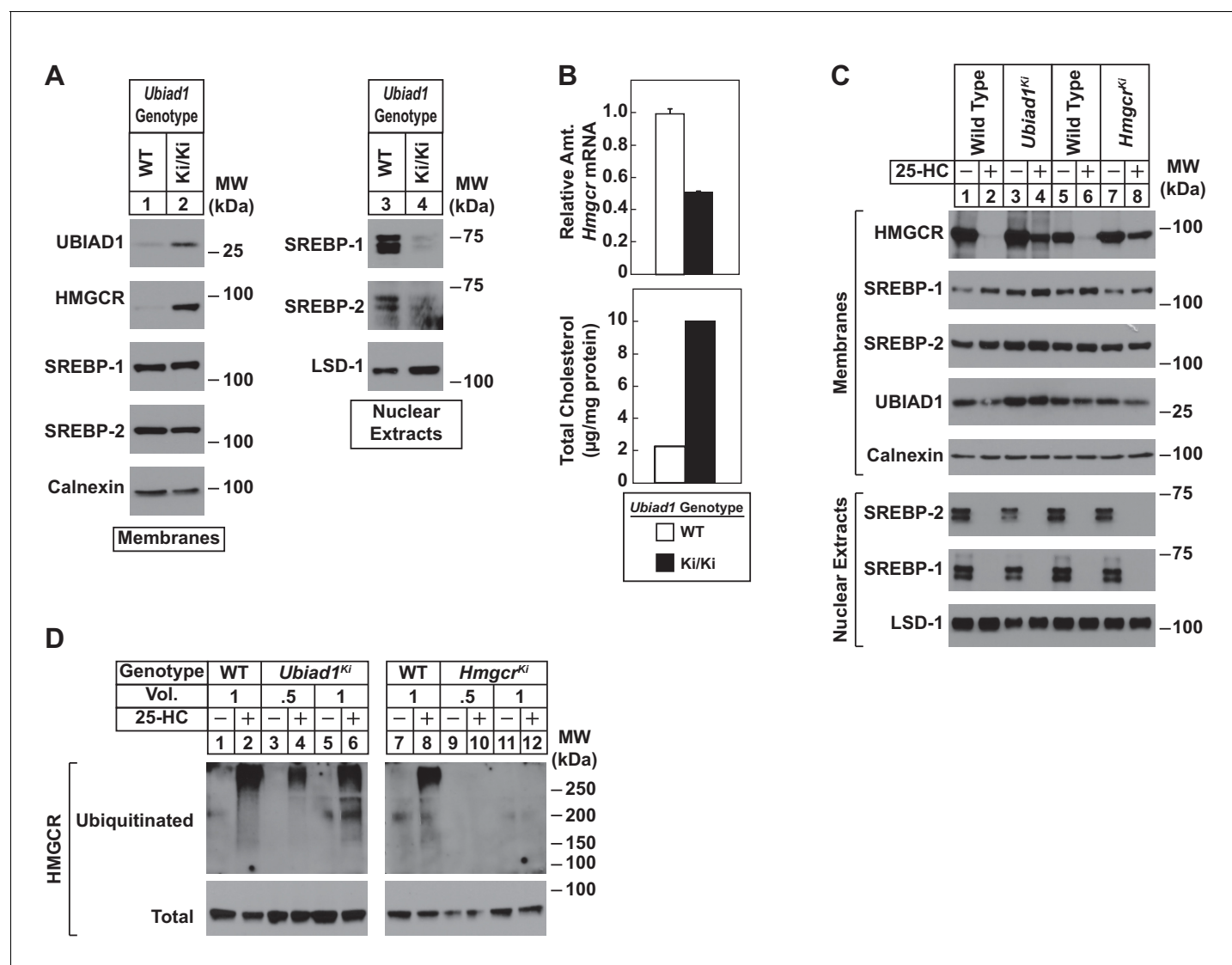
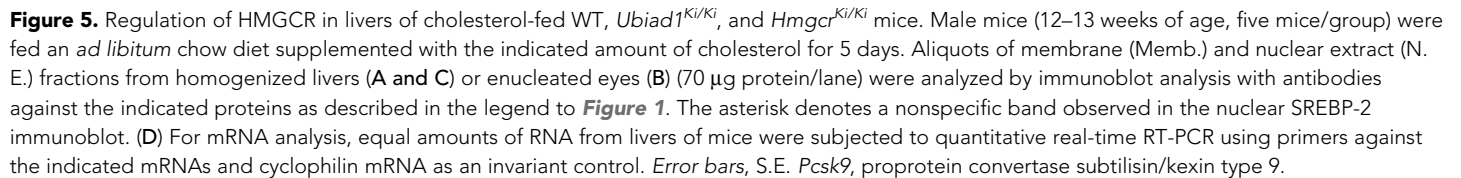


Figure 4. Sterol-mediated regulation of HMGCR in mouse embryonic fibroblasts (MEFs) from WT and *Ubiad1^{Ki/Ki}* mice. MEFs from WT and *Ubiad1^{Ki/Ki}* mice were set up for experiments on day 0 at 2×10^5 cells per 10 cm dish in MEF medium supplemented with 10% fetal calf serum (FCS). (A) On day 3, cells were harvested for subcellular fractionation. Aliquots of resulting membrane and nuclear extract fractions (35–50 µg total protein/lane) were subjected to SDS-PAGE, followed by immunoblot analysis using antibodies against the indicated proteins. (B) On day 3, cells were harvested for measurement of *Hmgcr* mRNA levels by quantitative RT-PCR and total cholesterol levels using a colorimetric assay as described in 'Materials and methods.' (C and D) On day 2, cells were depleted of isoprenoids through incubation for 16 hr at 37°C in MEF medium containing 10% lipoprotein-deficient serum, 10 µM sodium compactin, and 50 µM sodium mevalonate. The cells were subsequently treated with 1 µg/ml 25-HC as indicated; in (D), the cells also received 10 µM MG-132. (C) After 4 hr at 37°C, cells were harvested for preparation of membrane and nuclear extract fractions (35–50 µg total protein/lane) that were analyzed by immunoblot with antibodies against the indicated protein. (D) Following incubation for 1 hr at 37°C, cells were harvested, lysed in detergent-containing buffer, and immunoprecipitated with 30 µg polyclonal anti-HMGCR antibodies. Immunoprecipitated material was subjected to SDS-PAGE and immunoblot analysis with IgG-A9 (against HMGCR) and IgG-P4D1 (against ubiquitin).

DOI: <https://doi.org/10.7554/eLife.44396.009>



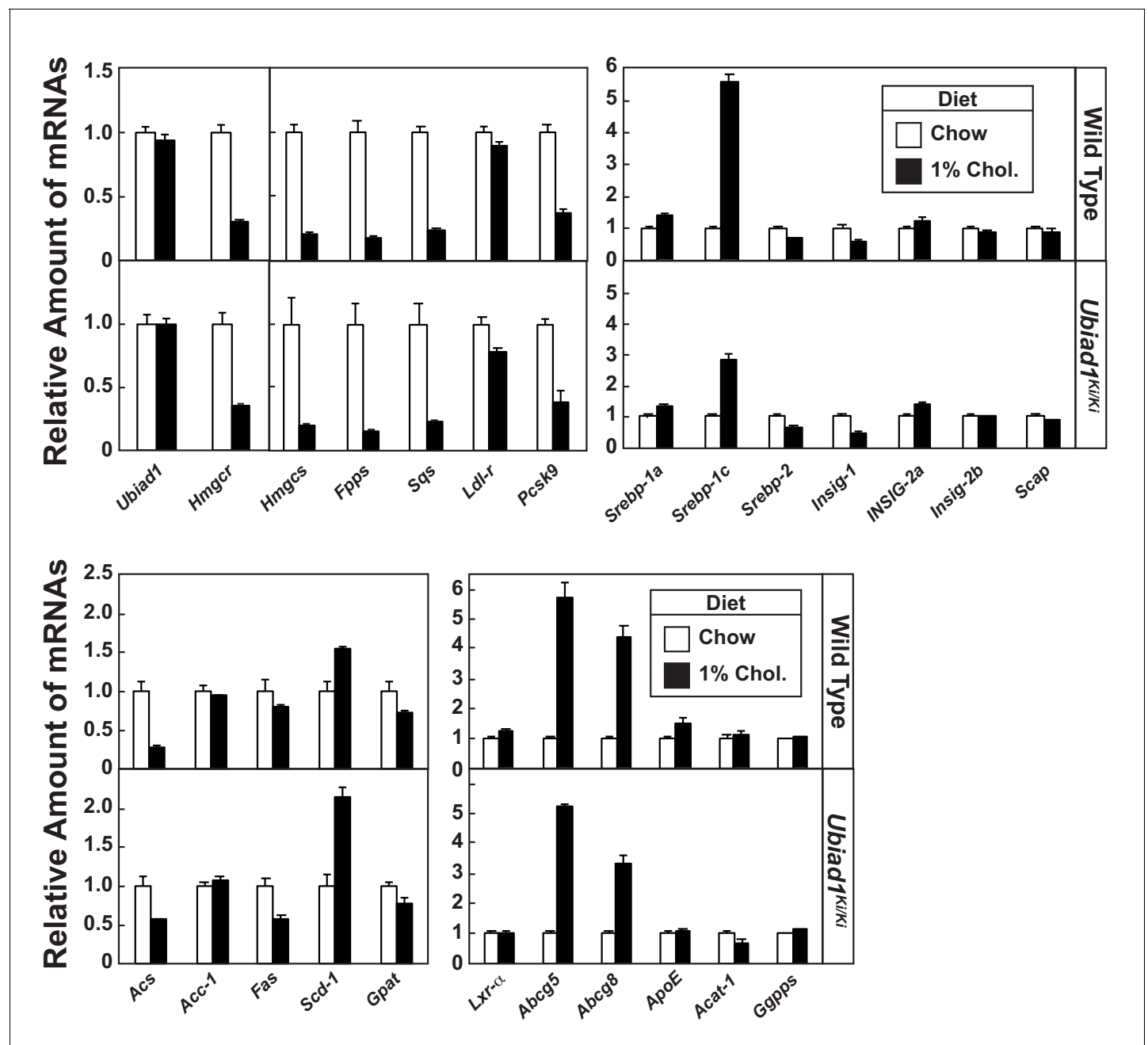


Figure 5—figure supplement 1. Effect of dietary cholesterol on expression of mRNAs encoding components of the Scap-SREBP pathway in livers of WT and *Ubiad1* knock-in mice. Total RNA from livers of mice used in **Figure 5A** (5 mice/group) was separately isolated. Equal amounts of RNA from the individual mice were subjected to quantitative real-time RT-PCR using primers against the indicated gene; cyclophilin mRNA was used as an invariant control. Each value represents the amount of mRNA relative to that in WT mice fed a chow diet, which was arbitrarily defined as 1. Bars, mean ± S.E. (error bars) of data from five mice. *ApoE*, apolipoprotein E; *Acat-1*, acyl-coenzyme A:cholesterol acyltransferase-1.

DOI: <https://doi.org/10.7554/eLife.44396.011>

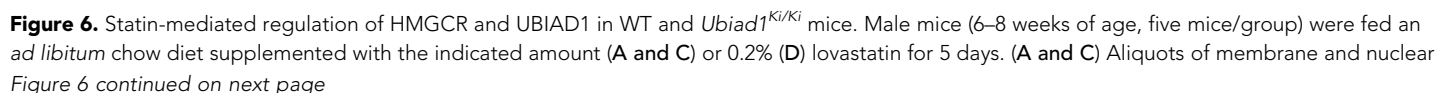


Figure 6 continued

extract fractions from homogenized livers (A) or enucleated eyes (C) (70 µg protein/lane) were analyzed by immunoblot analysis with antibodies against the indicated proteins. In (B), the amount of HMGCR protein in livers of *Ubiad1*^{Ki/Ki} mice shown in (A) was determined by quantifying the band corresponding to HMGCR using Image J software and normalizing to the amount of the protein in untreated WT controls. (D) Post nuclear supernatants (PNS) obtained from liver homogenates were fractionated on a discontinuous sucrose gradient (7.5–45%) that yielded a light membrane fraction enriched in Golgi and a heavy membrane fraction enriched in ER. Aliquots of the homogenates (lysate), nuclear extracts (N.E.), PNS, Golgi-enriched membranes, and ER-enriched membranes were subjected to SDS-PAGE, followed by immunoblot analysis with antibodies against the indicated proteins.

DOI: <https://doi.org/10.7554/eLife.44396.012>

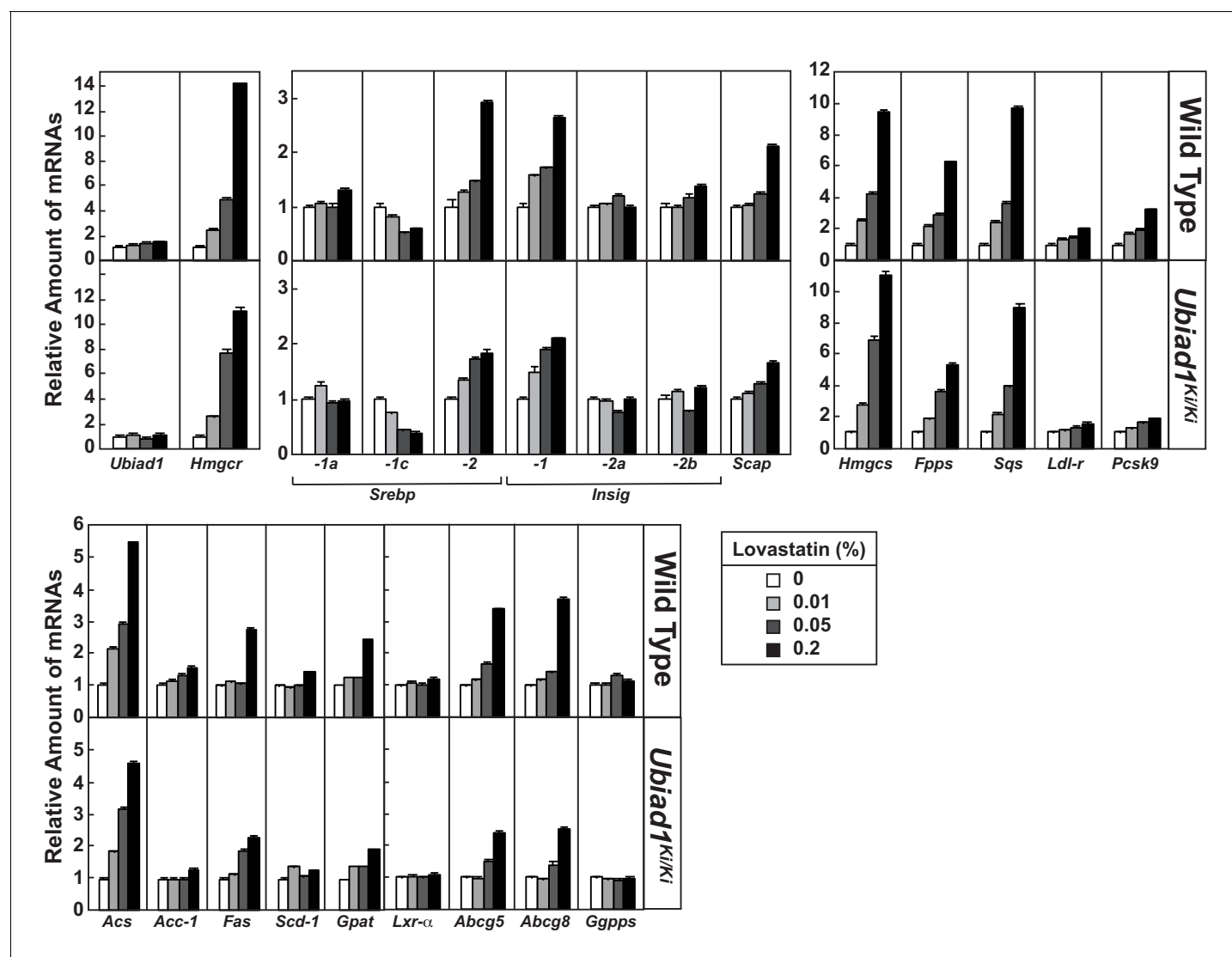


Figure 6—figure supplement 1. Effect of lovastatin on expression of mRNAs encoding components of the Scap-SREBP pathway in livers of WT and *Ubiad1* knock-in mice. Total RNA from livers of mice used in **Figure 6A** (5 mice/group) was separately isolated. Equal amounts of RNA from the individual mice were subjected to quantitative real-time RT-PCR using primers against the indicated gene; cyclophilin mRNA was used as an invariant control. Each value represents the amount of mRNA relative to that in WT mice fed a chow diet, which was arbitrarily defined as 1. Bars, mean \pm S.E. (error bars) of data from five mice.

DOI: <https://doi.org/10.7554/eLife.44396.013>

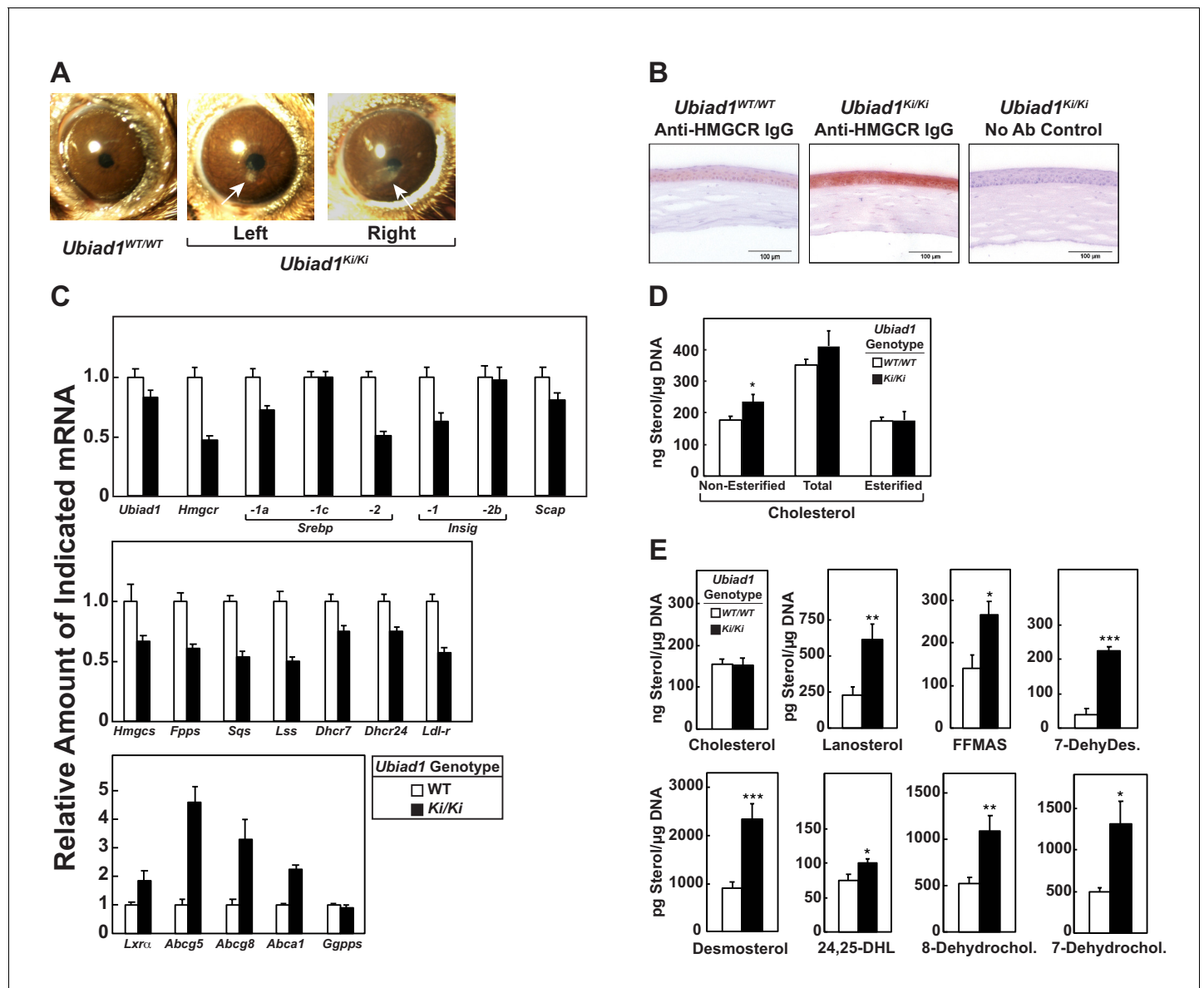


Figure 7. *Ubiad1*^{Ki/Ki} mice exhibit signs of corneal opacification upon aging. (A) Male and female mice (15 WT, 24 *Ubiad1*^{Ki/Ki}, 50 weeks of age) consuming an *ad libitum* chow diet were analyzed by stereomicroscopic examination. Corneal opacification is indicated by white arrows. (B–E) Mice analyzed in (A) were sacrificed, corneas were then harvested and analyzed by immunohistochemical staining with anti-HMGCR polyclonal antibodies (B), quantitative RT-PCR (C), and LC-MS/MS (D and E) as described in the legend to **Figure 1** and ‘Materials and methods.’ Error bars, S.E. The *p* value was calculated using Student’s *t* test: *, *p* < 0.05; **, *p* < 0.01; ***, *p* < 0.005. *Dhcr7*, 7-dehydrocholesterol reductase; *Dhcr24*, 24-dehydrocholesterol reductase; 7-DehyDes., 7-dehydrodesmosterol; 8-Dehydrochol., 8-dehydrocholesterol; 7-Dehydrochol., 7-dehydrocholesterol.

DOI: <https://doi.org/10.7554/eLife.44396.014>

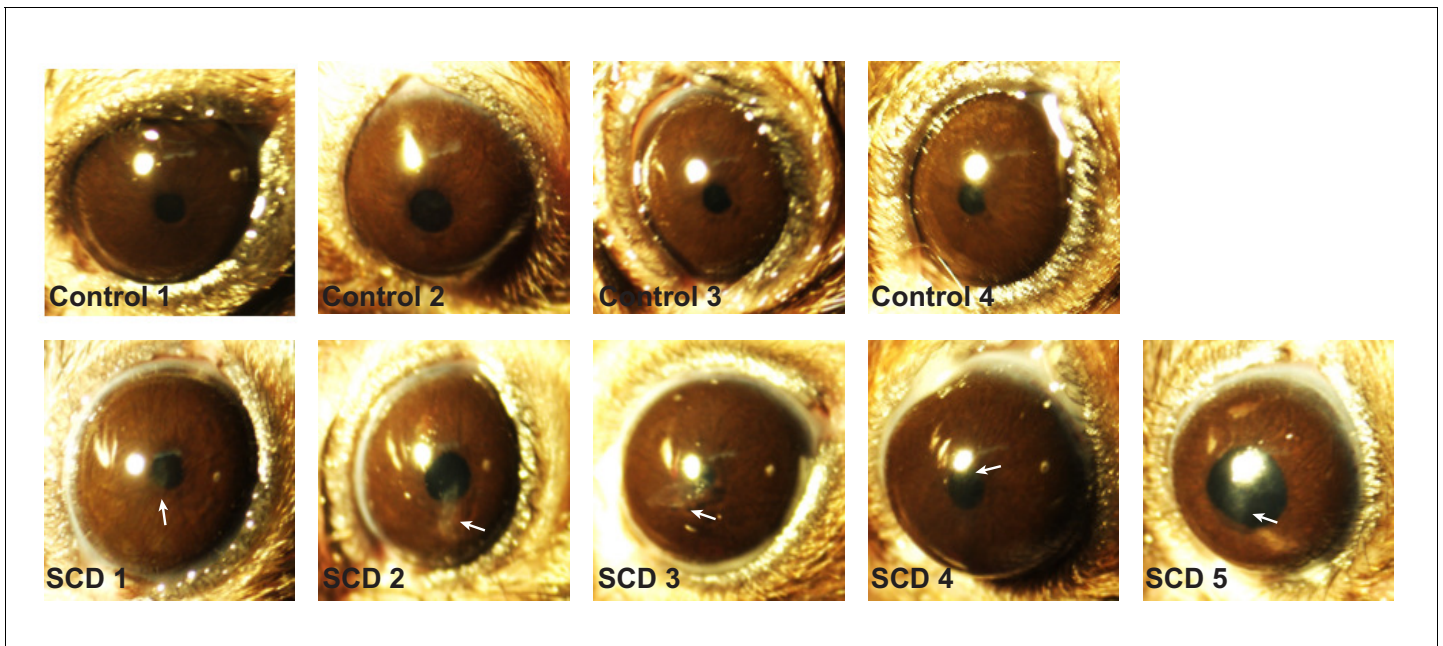


Figure 7—figure supplement 1. *Ubiad1*^{Ki/Ki} mice exhibit signs of corneal opacification upon aging. Female mice (15 WT, 24 *Ubiad1*^{Ki/Ki}, 50 weeks of age) consuming an *ad libitum* chow diet were analyzed by stereomicroscopic examinations as described in **Figure 7**. Corneal opacification is indicated by white arrows.

DOI: <https://doi.org/10.7554/eLife.44396.015>